Bataller Prats, R.; Gandía Romero, JM.; García Breijo, E.; Alcañiz Fillol, M.; Soto Camino, J. (2015). A study of the importance of the cell geometry in non-Faradaic systems. A new definition of the cell constant for conductivity measurement. Electrochimica Acta. 153(20):263-272. doi:10.1016/j.electacta.2014.12.014.

A study of the importance of the cell geometry in non-Faradaic systems. A new definition of the cell constant for conductivity measurment.

Roman Bataller[a,b], Jose Manuel Gandia[a,c], Eduardo Garcia[a,b], Miguel Alcañiz[a,b,*], Juan Soto[a,d].

[a] Centro de Reconocimiento Molecular y Desarrollo Tecnológico (IDM). Departamento de Química, Universitat Politècnica de Valencia. Camí de Vera, s/n. 46022 Valencia, Spain.

[b] Departamento de Ingeniería Electrónica, Universitat Politècnica de Valencia. Camí de Vera, s/n. 46022 Valencia, Spain.

[c] Departamento de Construcciones Arquitectónicas, Universitat Politècnica de Valencia. Camí de Vera, s/n. 46022 Valencia, Spain.

[d] Departamento de Química, Universitat Politècnica de Valencia. Camí de Vera, s/n. 46022 Valencia, Spain.

Abstract: A new definition for the electrochemical cell constant in conductivity measurements is presented in this paper. Electrochemical Impedance Spectroscopy and DC pulses measurements have been carried out in non-Faradaic conditions in order to evaluate the effects of the cell geometry. The results obtained demonstrate that conductivity measurements are affected not only by the electrodes surface and separation but also by the cross section of the electrochemical cell. In order to obtain a linear behavior of the resistance versus the distance between electrodes, the cross section of the cell should be equal to the electrodes surface. Differences between the cell cross section and the electrodes surface produce a heterogeneous distribution of the electric field that causes the non-linear behavior for low values of the electrodes separation. This study shows that the reproducibility in electronic tongue and humid electronic nose measurements can be improved by designing an electrochemical cell structure that warrants a homogeneous distribution of the electrical field, which results in a reduction of the detection threshold in these types of system.

KEYWORDS: conductivity; cell constant

1. Introduction.

The use of voltammetric techniques with electronic tongues and with some types of electronic noses combined with statistical analysis tools in the chemometrics discipline unfolds great opportunities for their application to non-destructive quality controls. This type of surveys is of great interest when online inspections are applied to complex systems, such as natural waters, sewage waters or many foodstuffs (drinks, milk, fruits, fish, meat, etc.). The importance of these techniques lies in that they can provide information about systems properties related to their composition or quality in a non-destructive, economic and fast manner.

A series of works devoted to the application of electronic tongues in several fields of great scientific and technical interest (environmental, food technology, warfare nerve agent gas detection, etc.) have been published in the last years.[1-3] In addition, a few prototypes have been developed, to mention one example a Wet Electronic Nose has been designed for the detection of vapors and gases.[4,5]

One of the most important difficulties in the development of electronic tongues and wet electronic noses, especially in solid sample systems (fruits, meats, fish, etc.), is the problematic reproducibility of the measurements.[6,7] These reproducibility problems can be caused by different factors:

i. Local variations of the resistivity in the samples. This is a common problem when heterogeneous solid materials (such as fruits, fish or meat) are measured with an electronic tongue. In the case of the Wet Electronic Nose, the reproducibility issues are probably caused by the reticular structure of the membrane (nylon, cotton, cellulose) supporting the absorbent liquid; the disposition of the fibers embedding the membrane is only anecdotally coincident onto the surface of the electrodes in consecutive measurements. According to our experience, the homogeneity of the applied electric field is a critical parameter for the success of this kind of applications.

ii. The geometry of the measurement cell. Parameters such as distance, surface and position of the electrodes and size and thickness of the sample are of great importance. The Fringe field effect plays a relevant role in the processes occurring during measurements.[8]

iii. Temperature. Temperature variations affect ionic mobility and therefore conductivity. An efficient thermostatic control is enough to assure experimental repeatability.

iv. Laminar or turbulent matter flow. Electrochemically active matter transport towards the electrodes provides higher current signals. Measurement techniques such as Rotating Disc Electrode (RDE) or Flow Injection Analysis (FIA) benefit from this effect.

In this paper the focus is set on the second factor, and in particular on how the performance of the three-electrode electrochemical cell used in electronic tongues and humid electronic nose can be affected by the cell geometry.

Two types of events can conduct electric current throughout an electrode-electrolyte interface. Non-Faradaic currents concern those events associated to the movement of electrolyte ions, adsorption and desorption processes, reorientation of solvent dipoles leading to the formation of the double layer or increasing it, etc. at the electrode-electrolyte interface; while Faradaic processes comprise direct transference of electrons caused by chemical reactions (oxidation at one electrode and a reduction at the other).

The use of a three-electrode configuration including a Working Electrode (WE), a Reference Electrode (RE) and an Auxiliary or Counter Electrode (AE/CE) in Electronic Tongues and Wet Electronic Noses systems warrant an accurate measurement of the Faradaic current (as the potential between the RE and the WE is kept constant). This potential is affected by the Ohmic drop of the system, a change in the position of the RE with respect to the WE produces a change in the non-Faradaic current. But there are other factors, as the electrodes surface and the sample size that affect this current. In two-electrode

configurations, a change in the distance between electrodes produces a dramatic variation in the non-Faradaic current of the system.

The study of how the cell geometry influences non-Faradaic current is of great importance when evaluating reproducibility problems in Electronic Tongue and Wet Electronic Nose systems.

For the purpose of simplicity a two electrode system has been used in this work to analyze and discuss from an electrochemical point of view the relation between cell geometry and non-Faradaic current.

In two electrode measurements charge circulation occurs when an electric field is applied between the two electrodes in contact with the sample. This electric field can produce Faradaic and non-Faradaic processes. The non-Faradaic processes are generally associated to the reorganization of the electrical double layer or the movement of ions inside the media. Faradaic processes are the result of the electron transfers between electrodes and ions or neutral species in the interfacial area (redox processes); they occur when oxidisable or reducible species reach the surface of an electrode whose surface electric potential is appropriate for the redox process.

When the electric conditions are suitable, for instance because the applied electric potential is small and/or of alternating current at medium or high frequencies, it can be considered that only non-Faradaic processes take place. The most direct information obtained when working in non-Faradaic conditions is the system's conductivity.

It was early proved that the conductivity of electrolytic solutions depends on the dissolved salt, its concentration and the dissociation degree. This behavior led since the end of the nineteenth towards the mid twentieth century to the use of alternating current to study the properties of electrolytic solutions. The period comprising 1920 and 1940 was the most productive time for the implementation of this technique and so for the results obtained, which allowed the development of the theoretical models that explain the behavior of electrolytic solutions nowadays.[9,10]

Over the time the use of classic conductometry has been losing relevance progressively due to the appearance of more advanced and versatile techniques such as impedance spectroscopy. However despite the amount of publications in this electrochemical area, conductometry is still widely used as an auxiliary control technique, essentially due to the low cost of the instruments and its wide application range. For instance, the measurement of the conductivity in potable, mineral or waste waters provides an idea of their content in salts; the control of conductivity in waste water treatment plants provides an idea of the evolution of the pollutant load during the physicochemical o biological purification processes. In food technology, the monitoring of conductivity is a very useful tool for composition control and also to control the salinity of brines used in processes such as fermentation, pickling, curing, etc.

Data obtained from electrochemical impedance spectroscopy (EIS) provides a lot more information than the gathered from a simple conductimeter which performs the measurements at a single frequency. This frequency scan makes up the frequency spectrum and its analysis permits to obtain useful information for the analysis and characterization of the system under study.

1.1. The use of equivalent circuits for the interpretation of solutions' behavior.

In the first works about conductivity determination of electrolytic solutions the usefulness of equivalent circuits was already demonstrated for a better understanding of their behavior.[9-11] The model generally accepted for the interpretation of the current flowing through a conductive solution where a Faradaic process occurs is shown in figure 1-A, and for non-Faradaic charge transport processes in figure 1-B.

Insert Figure 1

In this schematic circuits, C_{dl} represents the total capacity of the electrical double layer formed between the electrodes and the ions in the solution, R_Ω is the Ohmic resistance of the solution, R_p is the resistance of the redox electronic transfer and C_M is the macroscopic capacity associated to the

capacitive effects that take place between the working electrode and the auxiliary electrode immersed in the solution with a dielectric constant ε.

1.2. Conductivity cell-constant.

The determination of molar or equivalent conductivity of electrolytic solutions is done from the specific conductivity according to the expression:

$$\chi_T = \frac{\ell}{R_T \cdot S} \quad (1)$$

Where l is the distance between electrodes, R_T is the total resistance of the solution and S is the cross section of the ionic conductor. The quotient l/S is traditionally known as cell-constant (K).

However, it is a parameter which is rarely determined directly based on the physical dimensions of the electrochemical cell and the electrodes. This is traditionally justified because the surface of the commercial electrodes is very difficult to determine as they are usually platinized in order to obtain a much larger effective surface. Another reason is the edge effect on the electric field between the measurement electrodes.

There are many problems, some of them still have not been explained, in the determination of the cell-constant so it has to be done indirectly based on the resistive value of a pattern solution of KCl, whose resistivity is known. The ratio between the expected resistance and the real resistance allows the evaluation of the cell-constant l/S. For a better understanding of some aspects that have created some confusion and are still confusing, a small historical review is done for the concept "cell-constant".

Kohlrausch defined the cell-constant as a purely geometrical factor which was obtained directly from the quotient of the distance between the electrodes in the electrochemical cell and their surface area. In 1916 E. Washburn[12] in a paper devoted to the methodology in the measurement of electric conductivity

of solutions recommended the use of circular electrodes of similar diameter to the cylindrical deposit containing the solution whose conductivity is to be measured. By this time, both Washburn and Wien[13], interpreted the behavior of a solution by means of an equivalent circuit represented by a resistance and a series capacitor. This interpretation influenced significantly the design of first measurement devices which introduced a variable resistor and a variable capacitor in the measurement bridge to compensate the capacitance of the solutions.

In the period comprehended between 1922 and 1924, Parker published a series of works that contradicted the working methodology proposed by Kohlrausch, he showed that the cell-constant in the electrochemical cell had to be an apparent value, not real and presented a series of data showing that this value depended on the measured resistances of the solutions.[14,15] In a later work he proposed the use of cylindrical cells with diameters of electrodes and cells as alike as possible, by using several diameters of cell and different distances between electrodes.[16] The Geometric Cell Constant was calculated from the quotient l^2/V where l was the distance and V the volume of the cylindrical cell which was calculated by weighing the mercury that it contained.

In 1927, Randall and Scott[17] were working at a fixed frequency of 1000 Hz with four different electrolytes and two geometrically different conductivity cells and came to similar conclusions to Parker's. Between 1929 and 1931, Jones and Bollinger[18-20] present a series of works that coincide with Parker's proposal about the variations observed and demonstrate that different electrochemical cells show different values of conductivity. In order to avoid undesired parasitic capacitances they propose to separate the electrodes, increase the surface of the electrodes and platinize them so more reproducible results can be obtained. In addition, they showed that the conductivity variations with respect to the frequency did not present the importance that it had been attributed so far.

Another recognized electrochemist, Shedlovsky[11,21], between 1930 and 1932, obtained the conductivity of several salts at different frequencies to confirm the validity of data and detect erratic values while he built and checked many measurement cells designed with the aim of eliminating any effects that could disturb the measurement of conductance, specially polarization and adsorption. So he could state that immersion electrodes directly introduced in the problem solution are not appropriate due to reproducibility issues.

In the early fifties Randles made great contributions to the kinetics of electrode reactions[22], rate constants and activation energies of electrode reactions[23], electron exchange reactions[24], metal ion exchange reaction at amalgam electrodes[25] and many more publications. From these works the well-known equivalent Randles circuit was deduced, which is still widely used.

In the early sixties John Newman started a series works related with current distribution[26,27], limiting currents[28] and the development of the theory of electrochemical systems[29] that are ahead of the latest research improvements in this field.

Despite the great number of publications devoted to conductivity and cell constant determination there are still some non-linear behaviors in the conductivity measurements that have not been explained so far in the field of electronic tongues and noses. The understanding of all the phenomena related with non-Faradaic current in two electrodes configuration is a crucial factor to reduce the reproducibility problems when designing the measurement cell for Electronic Tongue and Wet Electronic Nose systems. In the present work different Impedance Spectroscopy and DC pulses studies have been carried out in order to analyze the non-linear behaviors in conductivity measurements and to understand how the geometry of the cell affects the non-Faradaic current.

2. Experimental.

2.1. Samples preparation.

Electrochemical studies were carried out using KCl, KNO_3 and Na_2SO_4 (of analytical grade and from Sigma-Aldrich) in water. Several KCl concentrations were analyzed: 3, 2.5, 2, 1, 0.75, 0.5, 0.25, 0.1, 0.01 and 0.001 molal. KCl has been used, as it is a traditional reference solution in conductivity measurements, in order to compare the data obtained in this work with the tabulated values found in bibliography. The concentrations studied for KNO3 and Na2SO4 were 1, 0.75, 0.5, 0.25, 0.1, 0.01 and 0.001 molal.

2.2. Electrodes.

All the measurements have been performed using the two electrodes measuring technique. The conductors used for the present study were electrodes of graphite, platinum, gold (which are commercial electrodes) and stainless steel (have been manufactured in the laboratory). Different surface sizes have been used:

- 0.0707 cm^2 for Au, Pt and C.
- 1.440 cm^2, 1.960 cm^2 and 5.474 cm^2 for stainless steel.

The electrodes of 0.0707 cm^2 surface are the tips used in the rotating disk electrode by Metrohm.

Several electrode morphologies have been used while defining the working conditions of the experiments. Squared, circular and ring shapes have been used in the preliminary tests. The stainless steel electrodes of 1.440 and 1.960 cm^2 surface cross sections were squared and the ones of 5.474 cm^2 were circular and almost equal to the total cross section of the larger electrochemical cell.

2.3. Electrochemical Cell.

Four different thermostated cells were made. A cylindrical geometry was used with internal diameters of 13.2 (Cell 1), 16.3 (Cell 2), 20.8 (Cell 3) and 26.9 (Cell 4) mm (corresponding cross sections of 1.368, 2.087, 3.398 and 5.683 cm^2 which were the available tube diameters found). The electrodes

described in section 2.2 were used in the designed cells. In all the measurements the pair of electrodes performing the test was of the same dimensions and material.

The electrochemical cells consist of two cylindrical bodies of approximately 50 cm each (see figure 2). The main body includes the thermostatic cell and it is built with two concentric tubes of a polymeric material (marked with parallel lines), which create a chamber in which the thermostating liquid flows from the circulating bath. In the bottom edge it can be placed any of the previously described electrodes (wired at WE1), which is immobilized with a female screw of the same polymeric material in the inner cylinder of the cell.

Insert Figure 2

In the upper part of the cell a T connection has been installed so a reserve thermostated deposit is connected. This reserve deposit contains the solution under study, so it refills the electrochemical cell as the mobile electrode (wired at WE2) displaces the solution in the measuring chamber while the measurements take place. The mobile electrode body is made with a cylinder of almost the same diameter as the measuring chamber, in which edge the corresponding electrode is attached. This mobile part can be displaced in a distance range between 0 and 40 cm approximately. The mobile part is fixed at the required distances with an external auxiliary element (if the tubes are similar enough no external fixing assistance is needed). The measurement of the separation between the electrodes is made with a precision of ±0.05 mm by using a Vernier caliper.

All the electrochemical measurements have been performed working in the described electrochemical cells at 25ºC. For the temperature control a refrigerated/heated circulating bath from PolyScience ® has been used, with a precision of ±0.005ºC.

2.4. Internal cross section determination of the electrochemical cell.

The internal cross section average of the electrochemical cell has been determined from the weight difference between the cell empty and filled with distilled water at 25ºC. The cell volume is then obtained from the quotient between the mass of the contained water over the density of the liquid at the working temperature. From the calculated volume and the known cell's length it can be determined the internal cross section of the cylindrical chamber. The determination of the parameter has been realized five times for each electrochemical cell prototype.

2.5. Electronic equipment.

As first measuring technique for the determination of the resistance of solutions it has been used Electrochemical Impedance Spectroscopy. A Metrohm Autolab B.V. potentiostat PGSTAT100 with a FRA2 module has been used for the performance of these measurements. The software application Nova, from Autolab as well, has been used for the data preprocessing and for the circuits fitting simulations.

For this study fifty frequency steps (logarithmic distribution) have been configured, from 1 MHz to 100 Hz with an AC perturbation with amplitude of 10 millivolts to minimize the occurrence of polarization phenomena. The noisy or erratic data have been discarded previously based on Kronig-Kramers analysis.[30] On the other hand, the impedance value at 10 kHz has been used as a rough approximation to the resistance value because at this frequency the observed capacitance values represent a minor component of the total impedance. For the data analysis the basic equivalent circuit has been discarded due to its inefficacy in the fitting of the experimental data.

As second measuring technique a commercial conductimeter (Crison GLP32) has been used. It has been previously calibrated with a series of known resistors. The device works with squared wave alternating current at 2500 Hz and 100mV amplitude. For this particular case (and based on the calibration) it has

been assumed that the inverse value of the measured conductance directly provides the resistance value of the solution under study.

The last measuring device used has been developed in the Centro de Reconocimiento Molecular y Desarrollo Tecnológico (IDM) to perform the pulse voltammetry measurements.[31]

The applied pulses had an amplitude of 10 mV and a duration of 2 ms for the least concentrated samples and 5 ms for the concentrations 1 m and above. Three consecutive pulses where applied and individual analyses of each pulse where performed to calculate the corresponding values of proposed circuit in figure 6. The parameters were fitted via iterative calculation using the Microsoft Excel tool Solver.

All the electrochemical measurements have been performed inside a Faraday cage at 25.0ºC.

3. Results and discussion.

According to the previously presented ideas, there is a series of problems which should be studied to fulfill the proposed objectives. In first place it is necessary to do a comparative analysis between the results of the different electrochemical techniques (pulse voltammetry and impedance spectroscopy), which can be combined when working with electronic tongues. This is why it is important to realize a comparative analysis of the behavior of the proposed equivalent circuits for the interpretation of the experimental results.

In second place, it is necessary to determine the most appropriate geometry for the measuring cell depending on the particularities of the system under study (solid, liquid, gas or vapor) and to be able to determine with accuracy the cell constant in order to normalize the results.

3.1. Electrochemical results analysis. Determination of the Ohmic resistance of electrolytic solutions by means of several measuring techniques.

The value of the electric resistance of an electrolytic solution can be conditional to the electrochemical technique employed in its determination. It is known that the response of solvated ions in the presence of an electric field depends on two factors: the magnitude of the electric field and its frequency if it is an oscillating wave.[32,33]

The resistivity is linear with the electric field when this field is small, which is the reason why in this study the working potentials are set to just a few millivolts. On the other hand the effect of the frequency on the resistivity of solutions has been described and discussed widely. It might be the reason to justify the possible differences between the obtained results for the electric resistivity when working with continuous or alternate measuring techniques. Another reason might be that the equivalent circuits employed for the calculation of the resistance are not the adequate for the analysis of the experimental data.

For the measurement of the conductivity in a non-Faradaic process the accepted equivalent circuit is the one shown in figure 1-B. For this equivalent circuit the impedance modulus is shown in equation 2:

$$|Z| = \sqrt{\frac{R_\Omega^2 + \left(\omega \cdot C_M \cdot R_\Omega^2 + \frac{1}{\omega \cdot C_{dl}} + \frac{C_M}{\omega \cdot C_{dl}^2}\right)^2}{\left(1 + \frac{C_M}{C_{dl}}\right)^2 + \omega^2 \cdot C_{dl}^2 \cdot R_\Omega^2}} \qquad (2)$$

And the phase angle for this model is shown in equation 3:

$$\phi = -\arctan\frac{Z''}{Z'} = -\arctan\left(\frac{-\left(\omega \cdot C_M \cdot R_\Omega^2 + \frac{1}{\omega \cdot C_{dl}} + \frac{C_M}{\omega \cdot C_{dl}^2}\right)}{R_\Omega}\right) \qquad (3)$$

Figure 3 displays the logarithmic variation of the impedance modulus figure (3-A) and phase (figure 3-B) versus the frequency of a KCl 3 molal solution at 25ºC and the corresponding simulation with equations 2 and 3 of the non-Faradaic equivalent circuit of figure 1-B.

Insert Figure 3

The differences between the theoretical and experimental results of the modulus and phase impedance versus frequency reveal that the first circuit is not appropriate.

It is again easy to demonstrate that the simplest equivalent circuits (figure 1) are not the most adequate for the simulation of electrolytic solutions. A double branched model formed by two parallel RC branches can be explained based on the independent migration process of ions and the formation of two electrical double layers on the electrodes' surfaces.

The proposed model is shown in figure 4-A, in which a double branch circuit has been used in order to consider independent ions migration and in which is further added an inductive element. It has been checked that the simulations improve significantly when an inductance L (LCR equivalent circuit) is included in the basic circuit. This is not a crazy idea because of the demonstrated existence of the magnetohydrodynamic effect.[34] The results improve noticeably compared to the simple circuits (figure 1) model, but yet do not present a satisfactory fitting as it can be seen in figure 4-B.

Insert Figure 4

However a better approximation is obtained by using an equivalent circuit $(RQL)C_M$ (see figure 5), where component Q is a constant phase element. This element is normally used to simulate the double-layer capacitance at solid electrodes by means of impedance spectroscopy studies, which usually show deviations from ideal behavior. This capacitance dispersion strongly depends on the state of the electrode's surface, its roughness and also on anion adsorption. The deviations from ideal capacitive

behavior can be empirically represented by the so-called CPE. [35] This model has been used to adjust the impedance spectra and obtaining the resistance value (R_Ω) of the studied solutions.

Insert Figure 5

For the realized tests applying DC pulses an $(RC)_2$ equivalent circuit (figure 6) has been used as model. The inductive component in the case of direct current signals is not relevant.

The resistance values have been calculated with Solver, a tool of Microsoft Excel. The charge/discharge equations (see equation 4) of the two parallel branches have been programmed to obtain the value of the four components of the circuit in figure 6 (two resistors and two capacitors; the total resistance is calculated as a parallel resistor).

$$i(t) = \frac{\Delta V}{R_+} e^{-t/R_+C_+} + \frac{\Delta V}{R_-} e^{-t/R_-C_-} \quad (4)$$

Insert Figure 6

The conductivity values of the samples measured with the commercial conductimeter have also been registered and so table I contains the measured values of the resistances obtained with the three just accounted techniques. The data contain the information of a set of KCl solutions of different concentrations at 25ºC measured with two platinum electrodes with a surface of 0.0707cm^2 separated 1cm in a cylindrical cell whose cross section was 1.368 cm^2. In the first column the modulus of the impedance at 10 KHz measured with EIS has been also introduced.

molality	|Z| (10KHz)	R (EIS)	R (DC pulses)	R (Cond.)
0.010	2261	2253	2265	2049
0.015	1502	1497	1509	1430

0.025	912.9	909.2	921.0	899.0
0.100	245.5	243.3	255.0	209.0
0.500	73.30	69.10	81.10	42.30

Table I: Resistance values of five KCl solutions at 25ºC by means of EIS, pulse voltammetry and conductometry.

The resistance values in table I for the different KCl solutions basically show that the obtained values depend on the used measurement technique. On the other hand, small excitation potentials are being used (10 mV for EIS and 10 mV in pulse voltammetry) with the intention of obtaining linear responses from the media, so the effect described by Wien about the variation of the resistivity in the presence of an electrical field does not manifest. Otherwise, although little variations of the resistance with the frequency seem to arise (Debye-Falkenhagen effect) it seems to have a minor effect because it is possibly mathematically encompassed by the constant phase element (Q).

3.2. Ohmic resistance of the ionic solutions over the distance between the electrodes.

Figure 7 shows the variation of the resistance value of a 0.250 m KCl solution at 25ºC from the data corresponding to the EIS measurements when using two platinum electrodes which surface is 0.0707 cm^2 and two stainless steel electrodes which surface is 5.474 cm^2 over the distance and in two different electrochemical cells (inner cross sections of 1.368 cm^2 and 5.683 cm^2 respectively).

Insert Figure 7

From this figure it can be observed that in some situations resistance is not linear with respect to distance, as equation 1 stands. In fact, in two of the represented data sets (symbols '□' and '●') an initial curvilinear section is displayed until almost 1 cm; the rest of the response is linear. Besides, the intercept extrapolating from the rectilinear section is considerably different from the zero value

proposed in this equation. Only the '△' symbols representation is linear and its intercept agrees with the expected behavior.

Moreover, it should be noted that the slopes of the data sets with symbols '●' and '△' are very similar, despite the electrodes surfaces considerably different (0.0707 and 5.474 cm^2). In this case the cross section of the measuring cell has to be pointed out to be responsible for this outcome, as in both cases it has been the same (5.683 cm^2).

On the contrary, the responses of the series represented by '□' and '●' are dissimilar although the same electrodes have been used. The difference in the cross section of the cells (1.368 and 5.683 cm^2) seems to be reason. According to these observations it is easier to confirm that the slopes of the rectilinear sections are an inverse function of the cross section of the electrochemical cells and independent of the surface of the electrodes.

Figure 8 represents the evolution of the resistance over the distance between the electrodes of three electrolytic solutions (0.100, 0.250 and 0.500 m KCl at 25ºC); measured in an electrochemical cell which cross section was 1.368 cm^2 and with two platinum electrodes whose surface was 0.0707 cm^2.

Insert Figure 8

Data in this figure show that when working in the same cell the slope in the linear section of the measured resistance over the distance between the electrodes is approximately an inverse function of the concentration of the electrolyte. It can also be observed that the extrapolated intercept of the rectilinear section also seems to obey this mathematical statement.

In table I it has been shown that the different electrochemical measurement techniques lead to similar resistance values, but not to the exact same results if the experimental error ranges of each of the techniques are considered. Figure 9 displays a detailed study of the evolution of the resistance of a 0.250

m KCl solution over the distance in a cell with a cross section of 1.368 cm^2 measured with two platinum electrodes (surface of 0.0707 cm^2) by means of Impedance Spectroscopy (10mV amplitude sinusoidal perturbation) and pulse voltammetry (with same amplitude). The models used for the data analysis have already been introduced in section 3.1. (EIS 1, EIS 2 and EIS3 modelled with the $(RQL)C_M$ equivalent circuit; and Pulse Voltammetry PV 1, PV 2 and PV 3 modelled with (RC)2 equivalent circuit).

Insert Figure 9

The data displayed in the figure show two well defined groups of resistance values versus the distance, which are separated about 20 Ohm. The obtained resistance values by means of EIS reveal smaller resistance values than those obtained from the pulse voltammetry technique. These differences seem to be caused by the relaxation effect, which appears at high frequencies. ~~the fact that with EIS the double layer is not completely formed by the majority of the scanned frequencies due to the alternating nature of the measuring signal~~. Nevertheless, the slopes within the linear sections are equal within the experimental errors, regardless of whether the measurement technique is of alternating or direct current basis.

The slope value is related to the total resistivity of the solution. Operating equation 1 and considering that the total resistivity of the solution is the inverse of the total conductivity, then:

$$\frac{\partial R_T}{\partial \ell} = \frac{\rho_T}{S} \qquad (5)$$

Therefore, the graphical representation of the measured resistance versus the distance in the linear section presents a slope equal to the total resistivity of the solution divided by the cross section of the cell. The slope values by means of EIS and pulse voltammetry are 24.114 $\Omega\ cm^{-1}$ and 24.096 $\Omega\ cm^{-1}$

respectively, which come to molar conductivity values of 122.48 and 122.57 S mol cm^{-1} which fit with the data found in the literature for the same sample (KCl 0.250 molal at 25ºC): 122.55 S mol cm^{-1}.

For the calculation of these two conductivity values of the KCl solutions, the following simplified expression has been used:

$$\Lambda = \frac{1000 \cdot \chi_{solute}}{C} \cong \frac{1000}{\rho_T \cdot C} = \frac{1000}{Slope \cdot S_c \cdot C} \qquad (6)$$

Where C is the molar concentration of solute and S_c is the cross section of the cell.

We would like to highlight that the non-linear response of the resistance of electrolytic solutions versus the distance shown in figures 7, 8 and 9 has not been described so far.

3.3. Cell constant.

According to figures 7, 8 and 9 the measured resistance when the electrodes are at a fixed distance (l > 0.75 cm) can be considered as the sum of two contributions: a resistance R_0 (which is the value of the obtained resistance at the intercept of the linear section) plus the contribution of the solution resistance under study R_l, which depends on the separation between electrodes and on the cross section of the cell. Figure 10 details these proposed arguments.

Insert Figure 10

According to figure 10, the following equation can be written:

$$R_T = R_0 + R_\ell \qquad (7)$$

It is obvious then that R_l can be related to the total resistivity of the solution with the distance between electrodes and the cross section of the conductive solution container, so the following expression can be written:

$$R_T = R_0 + \rho_T \cdot \frac{\ell}{S_c} = \left(R_0 \cdot S_c + \ell\right) \cdot \frac{\rho_T}{S_c} \qquad (8)$$

Figure 11 reveals the dependency of the intercept R_0 to the concentration of the electrolyte or resistivity of the solution. A systematic study about the determination of the connection between the slope (ρ_T/S_c) of the linear section of the solution's resistance and the intercept is shown in tables II and III.

	Cell 1		Cell 2	
molality	Slope(ρ/S_c)	Intercept	Slope(ρ/S_c)	Intercept
0.250	24.11	91.52	15.63	87.67
0.100	57.16	195.8	38.38	205.1
0.050	110.3	383.3	78.13	439.1
0.025	214.1	750.0	138.0	775.0
0.015	349.9	1230	228.2	1288
0.010	517.3	1835	337.7	1916

Table II: *Slope values of ρ/S_c and intercept for six KCl solutions at 25ºC in two cells of 1.32cm (cell 1) and 1.63cm (cell 2) in diameter and Pt electrodes of 3mm in diameter. Data obtained by means of EIS.*

	Na_2SO_4		KNO_3	
molality	Slope(ρ/S_c)	Intercept	Slope(ρ/S_c)	Intercept

1.000	1.900	0.2527	1.972	0.2839
0.500	3.045	0.2996	3.478	0.8124
0.250	4.994	0.6114	6.394	0.9480
0.100	10.69	0.7335	14.69	1.546
0.010	80.71	4.295	129.5	6.194
0.001	704.5	32.84	1135	48.73

Table III: *Slope values of ρ/S_c and intercept for six Na_2SO_4 and KNO_3 solutions at 25ºC in a cell of 2.69cm in diameter and Steel electrodes of 2.64 cm in diameter (Cell 4). Data obtained by means of EIS.*

Insert Figure 11

Experimental data present a linear increase of the intercept as a function of the solution's resistivity which leads to the following proposal: R_0 is directly proportional to the slope (ρ_T/S_c) and is dependent on the geometry of the cell (equation 8).

According to these data the cell constant only matches with the Geometric Cell Constant when the conductive cross section S_c (as H. H. Bauer discussed in the early seventies)[36], which contains the electrolytic solution, is equal to the surface of the electrodes (see figure 7). In this particular case, the resistance as a function of the distance is a straight line starting in the origin (zero intercept) and so zero is also the value of R_0. Several functions fulfill this condition. Some of the simplest include the subtraction of cross sections (S_c - S_e) or the subtraction of diameters (ϕ_c - ϕ_e). Some variations have been analyzed and the results show that the function that better explains the experimental behavior is the subtraction of the diameters inverse ($1/\phi_e - 1/\phi_c$).

Equation 9 considers this sections issue:

$$R_0 \cdot S_c = A \cdot S_c \cdot \left(\frac{1}{\phi_e} - \frac{1}{\phi_c} \right) = A \cdot S_c \cdot \frac{\phi_c - \phi_e}{\phi_e \cdot \phi_c} \qquad (9)$$

Where ϕ_c is the diameter of the cell and ϕ_e is the diameter of the electrode. In this equation, A is a constant whose value seems to be related to the geometry of the cell and electrodes. Combining equations 8 and 9, we obtain:

$$R_T = \left(A \cdot S_c \cdot \frac{\phi_c - \phi_e}{\phi_e \cdot \phi_c} + \ell \right) \cdot \frac{\rho_T}{S_c} \qquad (10)$$

Equation 10 is only valid for fitting the rectilinear section of the representation of the resistance versus the distance. For the particular case of the studied KCl solutions with a couple of Platinum electrodes of 0.0707 cm^2 in a cell of 1.368 cm^2, the slope is 3.5315 cm^{-1}. Since the difference of sections diameters ($1/\phi_e - 1/\phi_c$) is 2.575 cm^{-1}, A is equal to 1.0019 cm^{-1} by operating equation 10. For cells 1, 2 and 4, see table IV.

The calculated values for constant A are in practice coincident within the experimental error. In accordance to the average value of A, it can be proposed that for a cylindrical cell and circular electrodes the numerical value is 1.06 ± 0.08 cm^{-1}.

Cell	ϕe	ϕc	Sc	Slope	A
Cell 1	0.300	1.320	1.369	3.532	1.002
Cell 2	0.300	1.630	2.087	5.656	0.997
Cell 4	2.640	2.690	5.683	0.0467	1.167
Cell 4	2.640	2.690	5.683	0.0430	1.075

Table IV. *Constant A values obtained for the different cells.*

3.3.1. Cell Effective Constant for l >0.75 cm.

We can define the Cell Effective Constant (K_{ef}) as the sum of the Kohlrausch Geometric Cell Constant K, and the value of R_0 (y-intercept of the linear section extrapolation):

$$K_{ef} = A \cdot \frac{\phi_c - \phi_e}{\phi_e \cdot \phi_c} + \frac{\ell}{S_c} \qquad (13)$$

The difference between the K_{ef} and the geometrical value of the cell can be evaluated. For instance, for cell 1 if the couple of electrodes of 0.0707 cm^2 are separated 1cm K_{ef} is equal to 4.467 cm^{-1} (3.735 + 1/1.368), which is an intermediate value but very different from the Geometric Cell Constant when taking into consideration the cross section of the cell (1/1.368 = 0.731 cm^{-1}) or the quotient between the distance and the surface of the electrodes, which is 14.14 cm^{-1}. It is important to note that the value of the effective cell constant is applicable only when the distance between electrodes is greater than 0.75 cm (see Figure 10) which corresponds to the linear region of the resistance vs. distance graph.

Table V shows the molar conductivity values calculated from the slope of the linear section versus de distance. These values agree with the tabulated data of KCl conductivity values (within the experimental error rank).

molality	M	slope	Λ calc	Λ tab
0.500	0.4914	12.64	117.7	117.4
0.250	0.2476	24.11	122.5	122.7
0.100	0.0995	57.16	128.5	128.9
0.050	0.0498	110.3	133.1	133.3

0.025	0.0249	214.1	137.1	137.1
0.015	0.0150	349.9	139.3	139.7
0.010	0.0100	517.3	141.3	141.2

Table V: *ρ_T/S_c slope values; calculated molar conductivity in cell 2 (1.368 cm^2) and Pt electrodes of 3mm in diameter (data obtained by means of EIS) and tabulated molar conductivity for KCl at 25ºC.*

These results partially agree with the works published by Parker[15,16], who demonstrated that the known cell constant did not coincide with the geometrical value and which had an apparent value that found to be dependent on the solution's resistance. The results in this paper reveal that the dependency is linear and so can be included in the Effective Cell Constant.

3.3.2 Cell Effective Constant for l < 0.75 cm.

Finally, we try to study the region where the curvilinear variations of the resistance occur as a function of the distance, this is, the zone where the distance between electrodes is smaller than 0.75 cm. This is a relevant consideration in order to evaluate how the natural tendency in sensors miniaturization can affect the provided information reliability.

A simple empirical approach has been found by adding two terms to equation 10 which allows modeling the resistance variation at short distances without modifying the slope in the rectilinear zone. The proposed equation is:

$$R_T = R_I + \left(A \cdot \frac{\phi_c - \phi_e}{\phi_e \cdot \phi_c} \cdot \frac{B \cdot \ell}{1 + B \cdot \ell} + \frac{\ell}{S_c} \right) \cdot \rho_T \qquad (12)$$

Constants A and B can be determined by experimental fitting of the measured data to the model.

The calculated values for constant A are in practice coincident within the experimental error (1.025 cm^{-1}). In accordance to the average value of B, it can be proposed that for a cylindrical cell and circular electrodes of 0.3 mm of diameter, the numerical value is 12 ± 1 cm^{-1}.

Finally, the term R_I, which corresponds to the interfacial resistance or contact resistance, has been added. It justifies the shift in the resistance values of figure 9. The differences are probably caused because in the case of pulse voltammetry the double layer reaches a complete degree of organization imposed by the applied electric field. On the contrary, with EIS at working frequencies higher than 100 Hz this event does not manifest because there is not enough time to form the double layer at the interface. The results reveal that R_I depends on the measuring technique but it is reasonable to think that it may also depend on the solvent, the type of ion and its concentration. These aspects should be addressed in future research.

3.3.3. Electrodes geometry.

Finally, it has been studied how the change in shape of the working electrodes affect the measured resistances. Electrodes with two square cross sections (1.44 and 1.96 cm^2) have been used. However, the cells have been maintained in cylindrical shape (cells 3 and 4) which cell diameters are 2.09 and 2.69 cm. In order to apply equation 12 the value of R_I is assumed as zero and the diameter of the electrode is the diagonal length of the squared electrode. The dimensions used to calculate the difference in diameters are 1.697 and 1.980 cm respectively. Table VI includes the A and B values obtained by fitting the experimental data using equation 12 in the case of squared cross section electrodes.

Electrode (cm^2)	ϕcell (cm)	A (cm)	B (cm^{-1})
1.44	2.09	0.883	1.75
1.96	2.69	0.922	1.82

Table VI: *A and B values of the simulated response of a 0.25m KCl solution with two electrode-cell configurations.*

It is interesting to point out that for the employed cells constant A is close to 1 cm^{-1} when the electrodes are of circular shape. However when the electrode is squared A value is approximately 0.9 cm^{-1}.

Besides, it should also be noted that constant B, which is used to fit the first curvilinear section ($l < 0.75$ cm) has an approximate value of 1.8 cm^{-1}. This indicated that the shape and size of the electrode actively affects the value of constant B.

4. Conclusions.

1. - The calibration constant of an electrochemical cell coincides with the Geometric Cell Constant (l/S) when an electric field of homogenous direction is applied in the solution under study. This only occurs in the case of the electrodes surface and the cross section of the cell to be the same. When this condition is fulfilled, the graphic representation of the experimental resistance versus the distance is a straight line which intercept is zero.

2. - When the surface of the electrodes is smaller than the cross section of the cell the electric field lacks from directional homogeneity. In this situation the plot of the resistance vs. distance displays an initial curvature until it reaches about one centimeter to become linear afterwards.

In this second case, the slope of the rectilinear section is directly proportional to the resistance and inversely proportional to the cross section of the receptacle containing the solution under study. The obtained molar conductivity values of the KCl solutions by means of alternating current techniques agree (within the experimental errors) with the values obtained when applying a pulse potential of 10 mV.

3. - The exact measurement of the conductivity of electrolytic solutions requires an adequate design of the electrochemical cell. The ideal configuration is that the electrodes geometry matches the cell's cross section, that they are planar and parallel. They are to be fixed in a cell made of an insulating and inert material such as glass, Teflon or polyethylene. The cell should have small inlet and outlet in order not to alter the electric field homogeneity inside the cell.

4. - When the cell geometry cannot be optimal because of practical implications, it might convenient to use several electrodes to infer the slope of the resistance vs. distance evolution and the resistivity value can be calculated.

5. - According to our experience a design with moving electrodes turns out to be complex and fairly impractical for the use of electronic tongues and so further research on the development of an appropriate distribution of the electrodes in an electronic tongue should be done.

Acknowledgements:

Financial support from the Spanish Government (projects MAT2012-38429-C04-04 and IPT-2012-0069-310000) is gratefully acknowledged.

The pre-doctoral scholarship granted to Román Bataller Prats within the program "Formación de Personal Investigador (FPI) 2012" from Universitat Politécnica de Valencia is gratefully acknowledged.

References:

[1] "Electronic tongues and their analytical application" Y. Vlasov, A. Legin, A. Rudnitskaya. Anal. Bioanal. Chem. 373 (2002) 136-146.

[2] “Flow injection analysis applied to a voltammetric electronic tongue” F. Winquist, E. Rydberg, S. Holmin, C. Krantz-Rülcker, I. Lundström. Anal. Chim. Acta 471 (2002) 159-172.

[3] “A voltammetric electronic tongue as tool for water quality monitoring in wastewater treatment plants” I.Campos, M. Alcañiz, D. Aguado, R. Barat, J. Ferrer, L. Gil, M. Marrakchi, R.Martínez-Máñez, J. Soto, J.L. Vivancos. Water Res. 46 (2012) 2605-2614.

[4] “A humid electronic nose based on pulse voltammetry: A proof-of-concept design”. R. Bataller, I. Campos, M. Alcañiz, L. Gil-Sánchez, E. García-Breijo, R. Martínez-Máñez, L. Pascual, J. Soto, J. L. Vivancos. Sens. Actuator B-Chem. 186 (2013) 666-673.

[5] A “humid electronic nose” for the detection of nerve agent mimics; a case of selective sensing of DCNP (a Tabun mimic). L. Pascual, I. Campos, R. Bataller, C. Olguín, E. García-Breijo, R. Martínez-Mañez, J. Soto. Sens. Actuator B-Chem. 192 (2014) 134-142.

[6] “Accurate concentration determination of anions nitrate, nitrite and chloride in minced meat using voltammetric electronic tongue”. I. Campos, R. Masot, M. Alcañiz, L. Gil, J. Soto, J. L. Vivancos, E. Garcia-Breijo, R. H. Labrador, J. M. Barat, R. Martínez-Máñez. Sens. Actuator B-Chem. 149 (2010) 71-78.

[7] “Acquisition and Analysis of Cyclic Voltammetric Data”. P. E. Whitson, H. W. Vanderborn, D. H. Evans. Anal. Chem. 45 (1973) 1298-1305.

[8] “Electric field outside a parallel plate capacitor”. G. W. Parker. Am. J. Phys. 70 (2002) 502-507.

[9] “Zur Theorie der Elektrolyte”. P. Debye, E. Hückel. Physik. Zeitschr. 9 (1923) 185-206.

[10] “The interionic attraction, theory of electrical conductance”. J. Warren Williams, H. Falkenhagen. Chem. Rev. 6 (1929) 317-345.

[11] “The electrolytic conductivity of some univalent electrolytes in water at 25ºC”. T. Shedlovsky, J. Am. Chem. Soc. 54 (1932) 1411-1428.

[12] “The measurement of the electrolytic conductivity. I .The theory of the design of conductivity cells”. E. W. Washburn. J. Am. Chem. Soc. 38 (1916) 2431-2460.

[13] “Über eine Abweichung vom Ohmschen Gesetze bei Elektrolyten”. M. Wien. Ann. Phys. 388 (1927) 327-361.

[14] “The calibration of cells for conductance measurements”. C. A. Kraus, H. C. Parker. J. Am. Chem. Soc. 44 (1922) 2422-2428.

[15] “The calibration of cells for conductance measurements. II . The comparison of cell constants”. H. C. Parker, J. Am. Chem. Soc, 45 (1923) 1366-1379

[16] “The calibration of cells for conductance measurements. III. Absolute measurements on the specific conductance of certain potassium chloride solutions.” H. C. Parker, E. W. Parker. J. Am. Chem. Soc. 46 (1924) 312-335.

[17] “The variation of the cell constant with concentration and the molal conductance of aqueous Barium Nitrate, Sodium Sulfate and Sulfuric acid at 0ºC”. M. Randall, G. N. Scott, J. Am. Chem. Soc. 49 (1927) 636-647.

[18] “The measurement of the conductance of electrolytes. II. Improvements in the oscillator and detector”. G. Jones, G. M. Bollinger, J. Am. Chem. Soc. 51 (1929) 2407-2416.

[19] “The measurement of the conductance of electrolytes. III. The design of cells”. G. Jones, G. M. Bollinger, J. Am. Chem. Soc. 53 (1931) 411- 451.

[20] “The measurement of the conductance of electrolytes. V. The validity of Ohm's law for electrolytes”. G. Jones, G. M. Bollinger, J. Am. Chem. Soc. 53 (1931) 1207–1212.

[21] “A conductivity cell for eliminating electrode effects in measurements of electrolytic conductance”. T. Shedlovsky. J. Am. Chem. Soc. 52 (1930) 1806-1811.

[22] “Kinetics of rapid electrode reactions”. J.E.B. Randles, Discuss. Faraday Soc. 1 (1947) 11-19.

[23] “Kinetics of rapid electrode reactions. Part 2.- Rate constants and activation energies of electrode reactions”. J. E. B. Randles, Trans. Faraday Soc. 48 (1952) 828-832.

[24] “Kinetics of rapid electrode reactions. Part 3.- Electron exchange reactions”. J. E. B. Randles, K. W. Somerton, Trans. Faraday Soc.48 (1952) 937-950.

[25] “Kinetics of rapid electrode reactions. Part 4.- Metal ion exchange reaction at amalgam electrodes”, J. E. B. Randles and K. W. Somerton, Trans. Faraday Soc. 48 (1952) 951-955.

[26] “Theoretical Analysis of Current Distribution in Porous Electrodes”, J. S. Newman and C. W. Tobias, J. Electrochem. Soc. 109 (1962) 1183-1191.

[27] “Engineering Design of Electrochemical Systems”, J. S. Newman. Industrial & Engineering Chemistry, 60 (no. 4, April, 1968), 12-27.”

[28] “Double Layer Structure at the Limiting Current”, W. H. Smyrl and J. S. Newman. Trans. Faraday Soc. 63 (1967) 207-216.

[29] “Electrochemical Systems”, J. S. Newman and K. E. Thomas-Alyea. 3rd edition. Hoboken, N. J.: Wiley-Interscience, 2004.

[30] “Application of the Kramers Kronig Relations in Electrochemical Impedance Spectroscopy,” P. Agarwal, M. E. Orazem, L. H. García-Rubio. Electrochemical Impedance: Analysis and Interpretation, ASTM STP 1188, J. Scully, D. Silverman, M. Kendig. American Society for Testing and Materials, Philadelphia, 1993, 115-139.

[31] “Diseño de un sistema de lengua electrónica basado en técnicas electroquímicas voltamétricas y su aplicación en el ámbito agroalimentario”. M. Alcañiz. Ph. D. Thesis. Universitat Politècnica de València (2011).

[32] “The Wien Effect: Deviations of Electrolytic Solutions from Ohm's Law under High Field Strengths”. H. C. Eckstrom , C. Schmelzer . Chem. Rev. 24 (1939) 367–414.

[33] “Frequency dependence of ionic conductivity of electrolyte solutions”. A. Chandra, B. Bagchi. J. Chem. Phys. 112 (2000) 1876-1886.

[34] “An AC magnetohydrodynamic micropump”. A. V. Lemoff, A. P. Lee. Sens. Actuator B-Chem. 63 (2000) 178-175.

[35] “Impedance Spectroscopy: Theory, Experiment and Applications”. E. Barsuokov, J. R. Macdonald. Wiley-Interscience. 2005.

[36] “Electrodics: modern ideas concerning electrode reactions”. H. H. Bauer, Thieme editions in chemistry and related areas, 1972.

Figures:

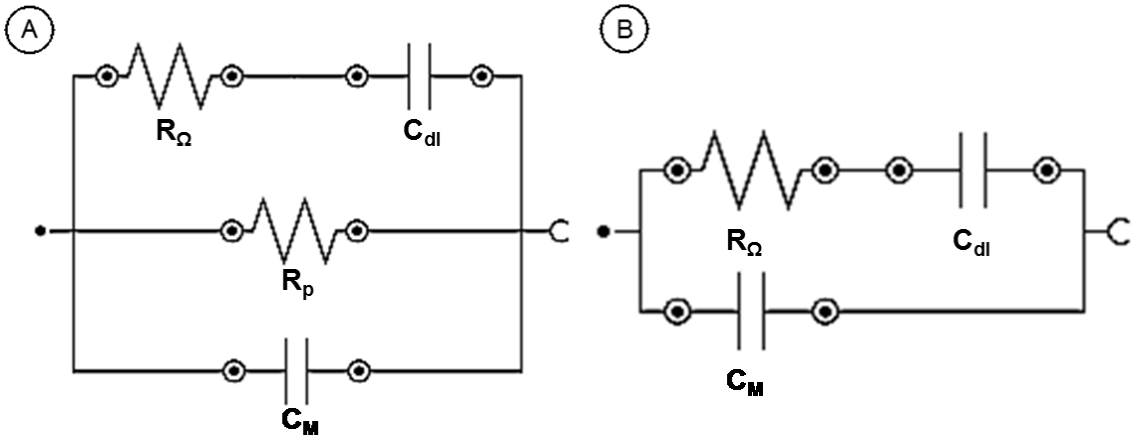

Figure 1: *Equivalent circuits of an electrolytic solution: 1-A (left), Faradaic process, 1-B (right) non-Faradaic process.*

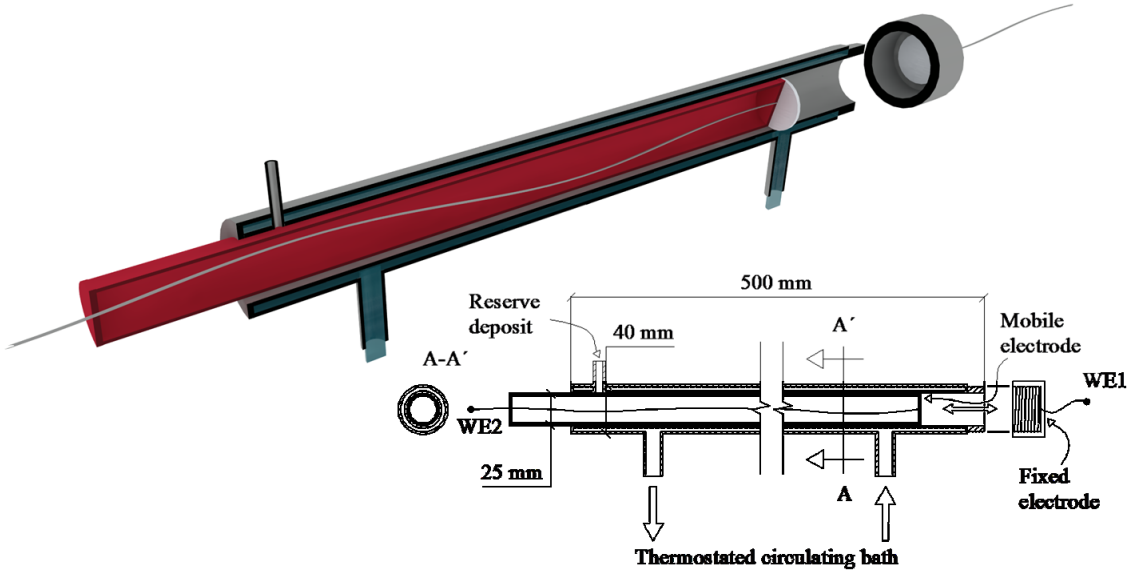

Figure 2: *Conductivity cell 4 diagrams (horizontal view).*

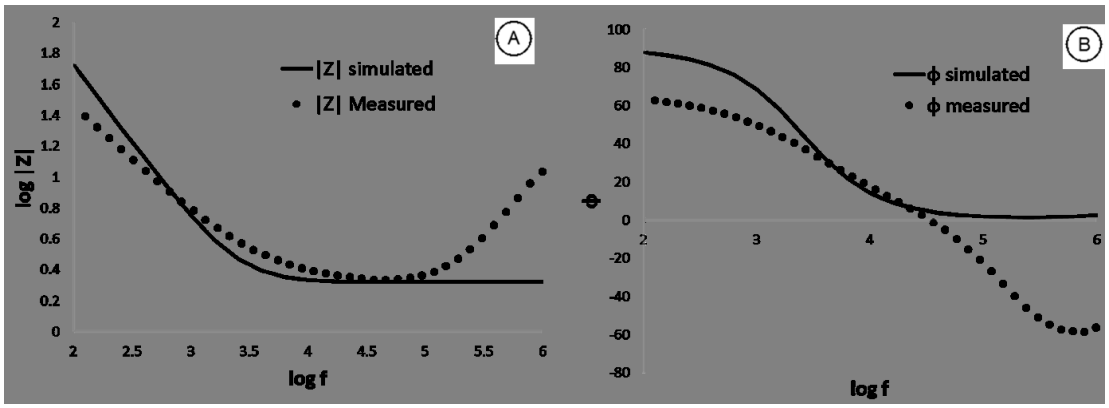

Figure 3: *log Z and phase for a KCl 3 m solution at 25ºC. 3-A: logarithm of the modulus and the simulated modulus (continuous line); 3-B: logarithm of the phase and simulated phase (continuous line).*

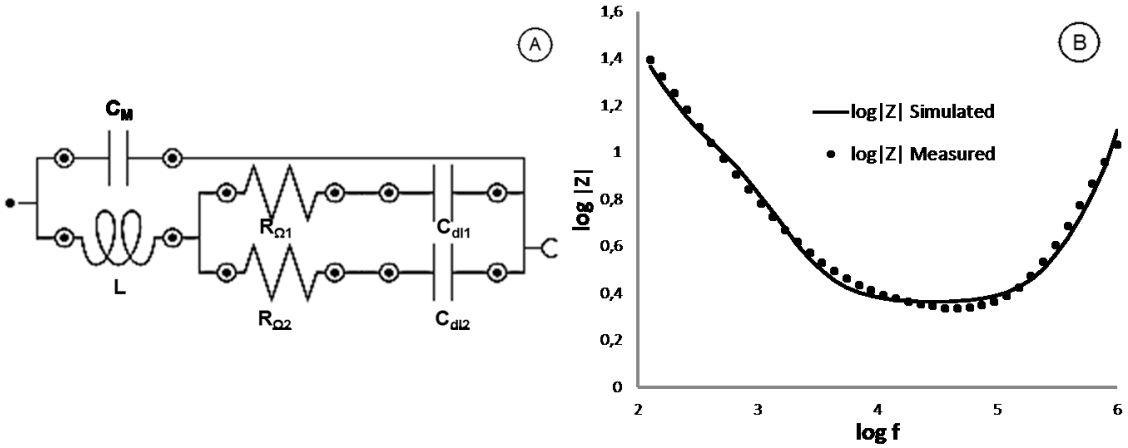

Figure 4: *Logarithm of the impedance spectrum of a KCl 3 molal solution (points) and the model fitting (continuous line) (figure 4-B) separated 3cm by using the equivalent circuit in figure 4-A.*

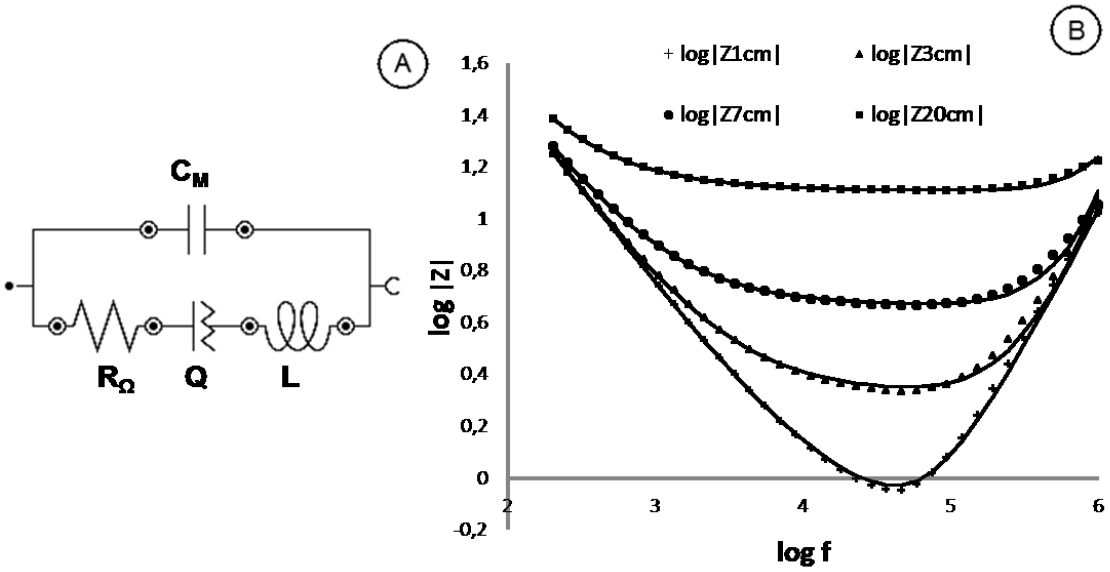

Figure 5: *Logarithm of the impedance spectrum of a KCl 3 molal solution (points) and the model fitting (continuous line) figure 5-B at 1, 3, 7 and 20 cm by using the equivalent circuit (RQL)C_M in figure 5-A.*

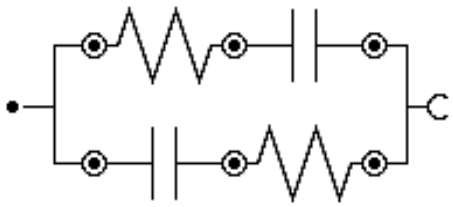

Figure 6: *equivalent circuit $(RC)_2$ for the analysis of the intensity vs. time response when applying a DC pulses.*

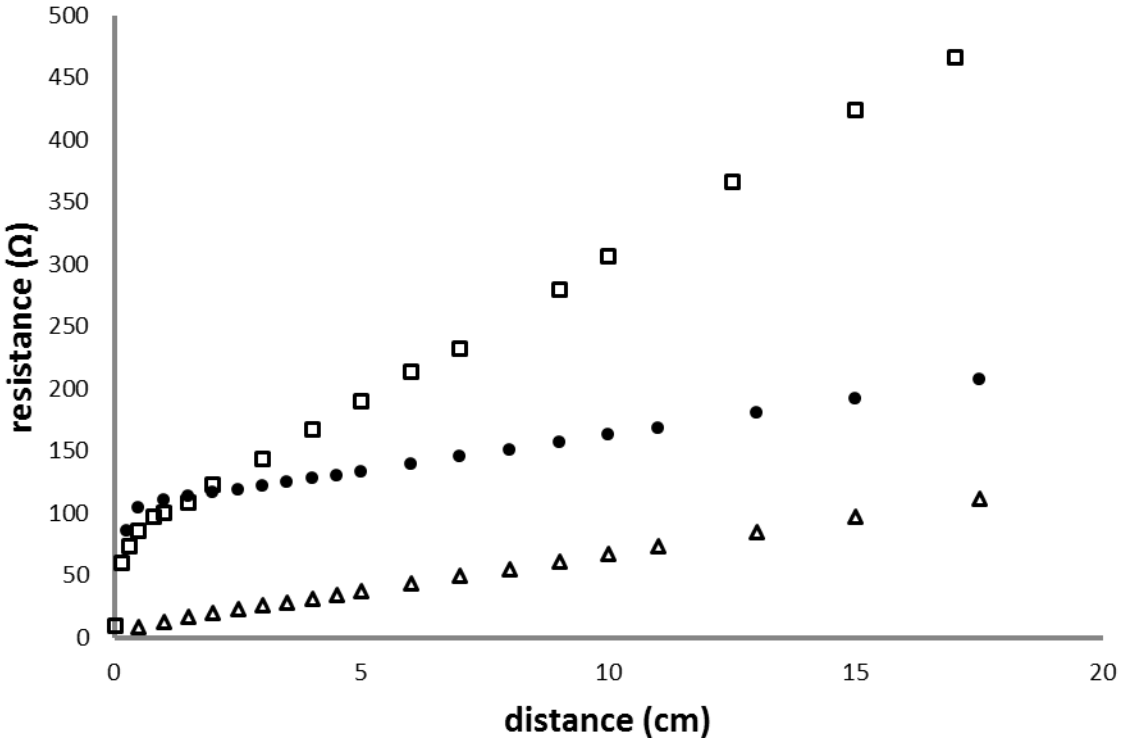

Figure 7: *resistance vs. distance graph of a 0.25 m KCl solution and three electrode-cell configurations (□ electrode surface 0.0707 cm^2, cell cross section 1.368 cm^2; ● electrode surface 0.0707 cm^2, cell cross section 5.683 cm^2; △ electrode surface 5.474 cm^2, cell cross section 5.683 cm^2) with EIS at 10 kHz.*

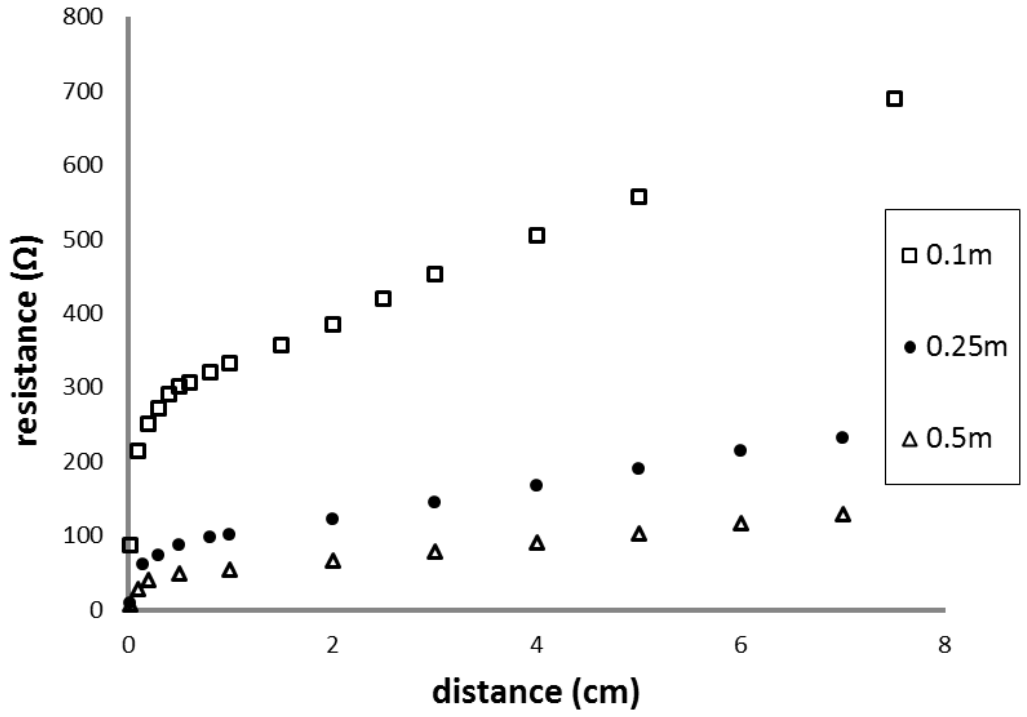

Figure 8: *resistance vs. distance graph of three KCl solutions (0.100, 0.250 and 0.500 m) in a cell with a cross section of 1.368 cm^2 measured with two platinum electrodes (surface of 0.0707 cm^2) with EIS at 10 kHz.*

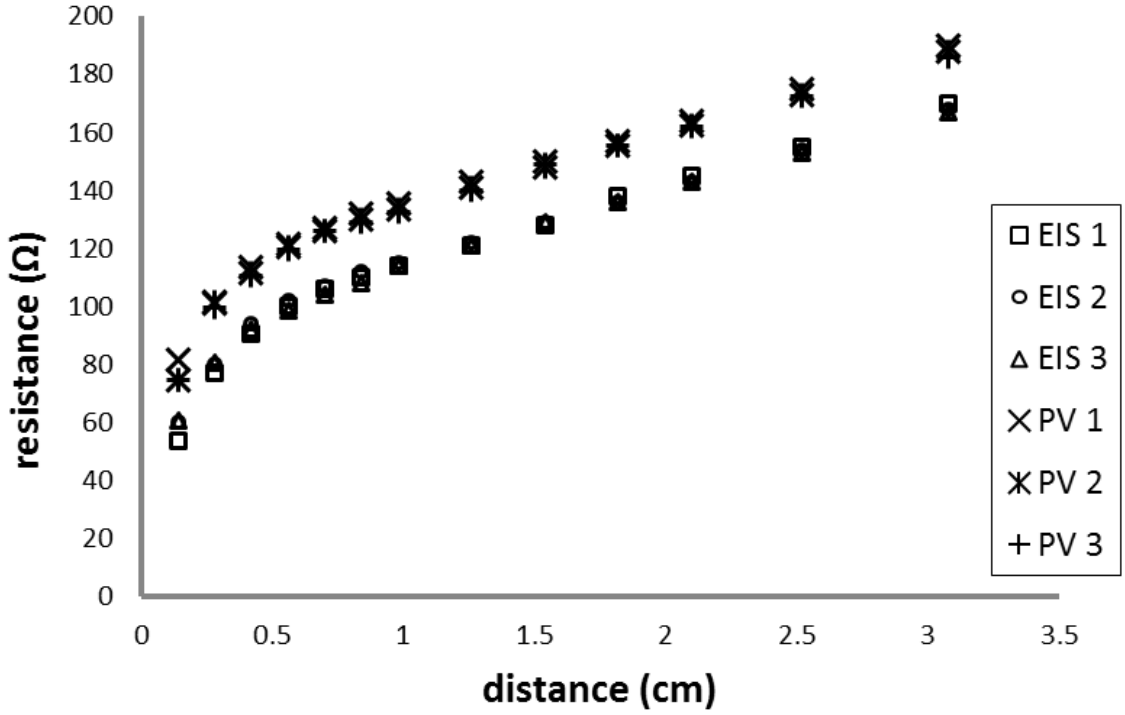

Figure 9: *resistance vs. distance graph of a 0.250 m KCl solution in a cell with a cross section of 1.368 cm^2 measured with two platinum electrodes (surface of 0.0707 cm^2) by means of EIS and PV at 25.0ºC.*

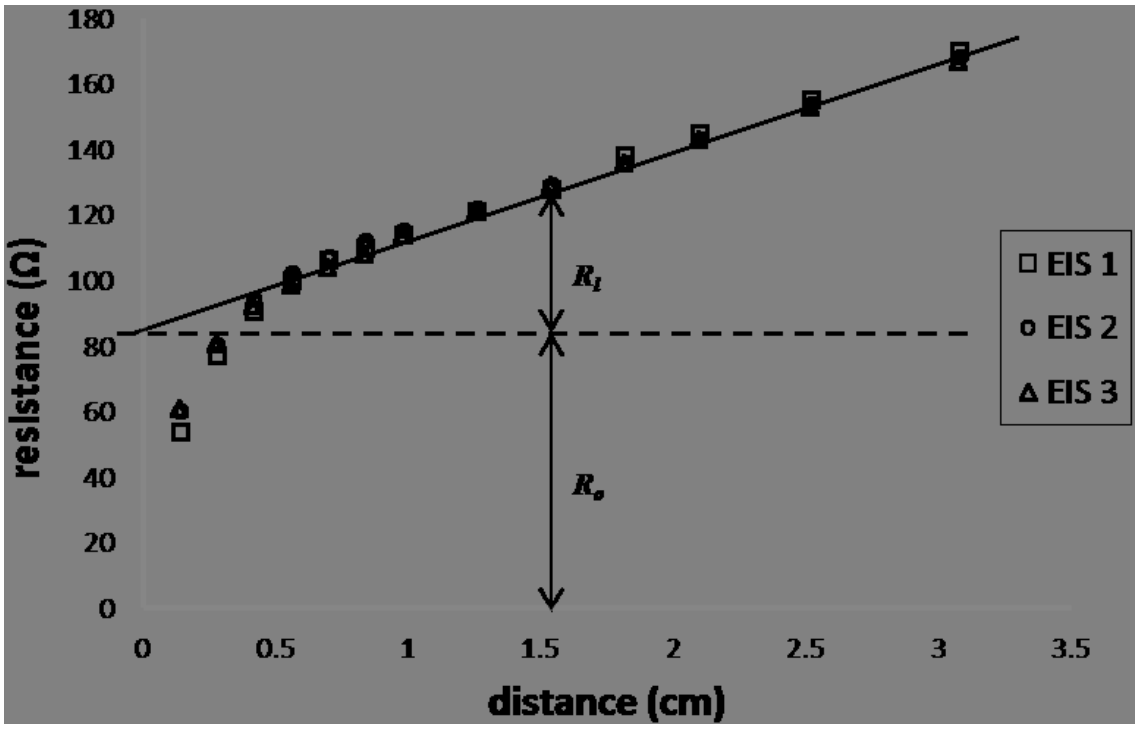

Figure 10: *R_0 and R_l definitions referred to the total measured resistance.*

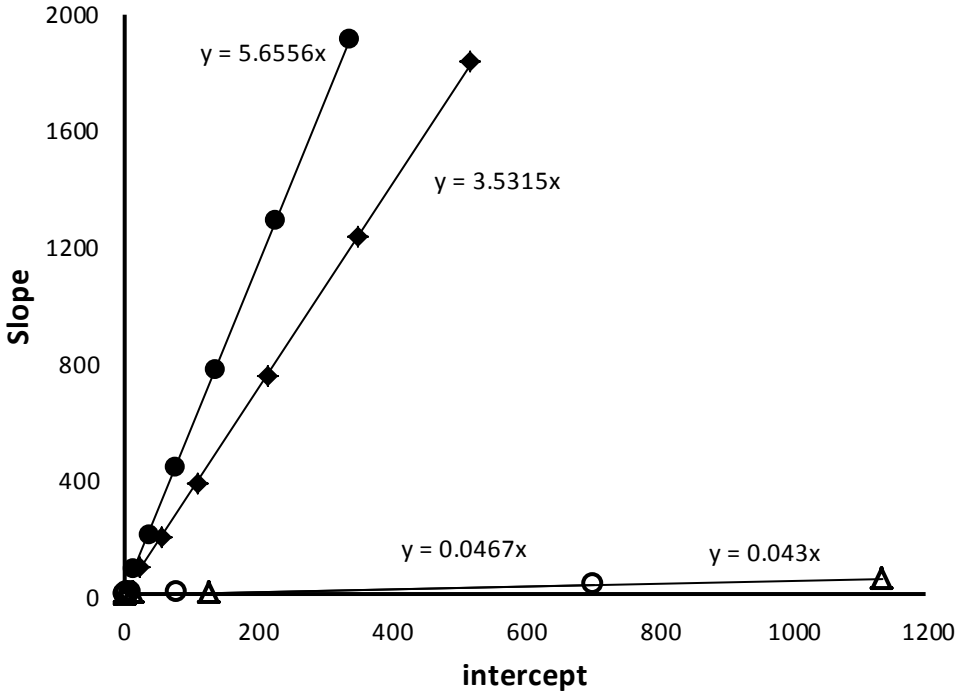

Figure 11: *Intercept versus slope plot of the resistance variations versus the distance (● KCl, electrode diameter 3 mm, cell 2; KCl, ◆ electrode diameter 3 mm, cell 1; KNO_3, △ electrode diameter 2.64, cell 4; ○ Na_2SO_4, electrode diameter 2.64, cell 4).*